Electronic Supplementary Material (ESI) for Journal of Materials Chemistry C.

Supporting Information

Rapid preparation of self-supported nickel-iron oxide as a high-performance glucose sensing platform

Ming Ni,[a,b,†] Minyuan Tan,[b,†] Ying Pan,[c] Chuhong Zhu,[a,*] and Haiwei Du[a,*]

[a] *School of Materials Science and Engineering, Anhui University, Hefei 230601, China*

[b] *School of Chemistry and Chemical Engineering, Anhui University, Hefei 230601, China*

[c] *School of Chemical Engineering, The University of New South Wales, NSW 2052, Australia*

Corresponding author emails:

chzhu@ahu.edu.cn (C. Zhu)

haiwei.du@ahu.edu.cn (H. Du)

[†] These authors contributed equally to this work.

Figure S1 Photographs of bare NF, NiFeO$_x$–600/NF, and NiFeO$_x$–800/NF.

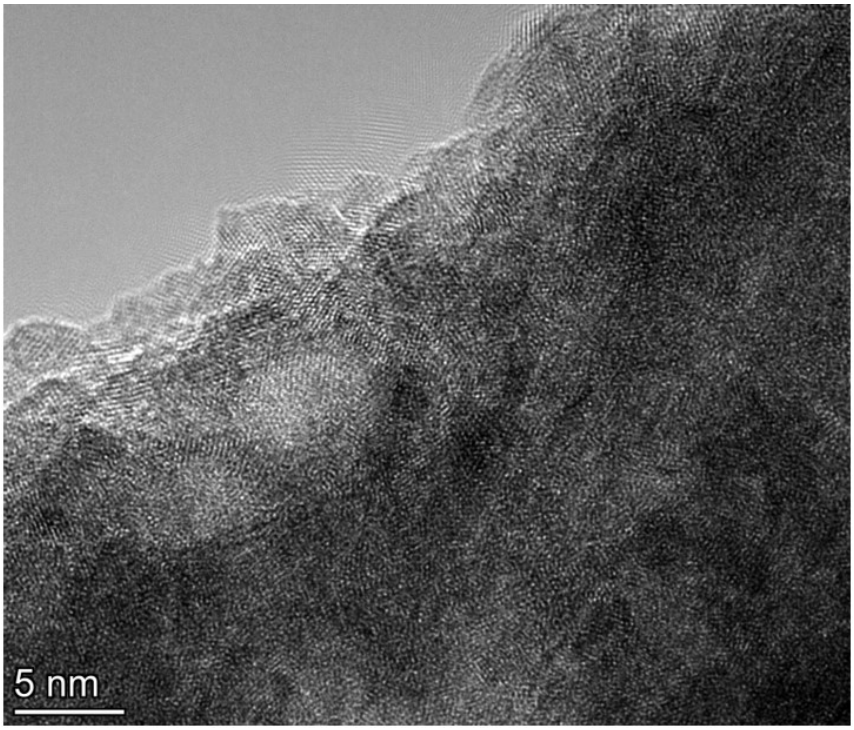

Figure S2 HRTEM image of NiFeO$_x$–800 powder sample, which was peeled off from the nickel foam substrate. The lattice fringe corresponds to crystalline domains.

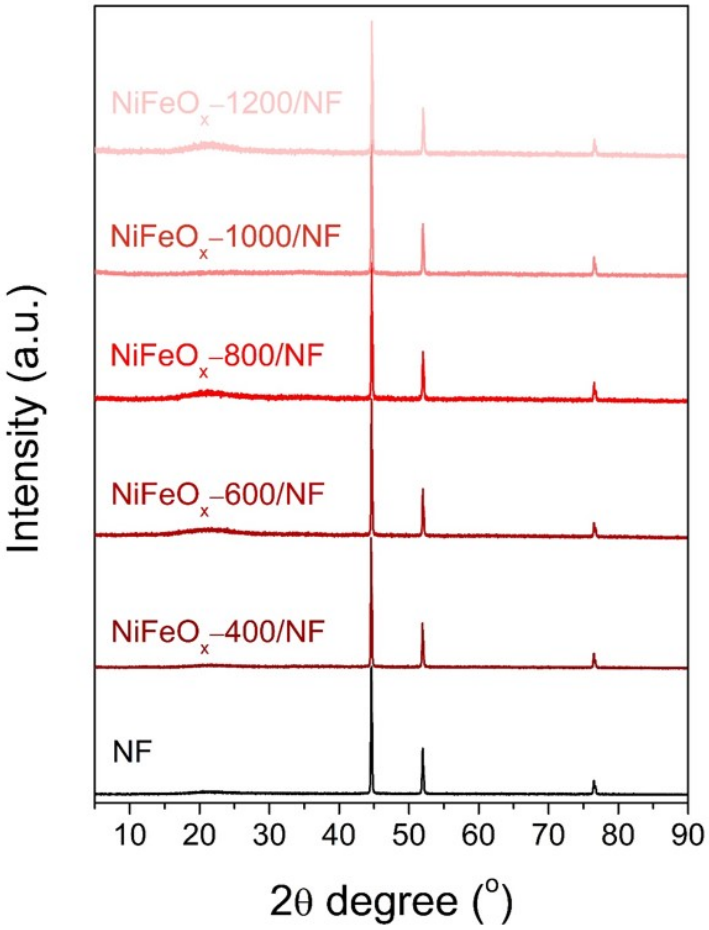

Figure S3 XRD patterns of NiFeO$_x$–*t*/NF prepared via different electrodeposition time.

Three main peaks are assigned to nickel foam, indicating that NiFeO$_x$ is amorphous.

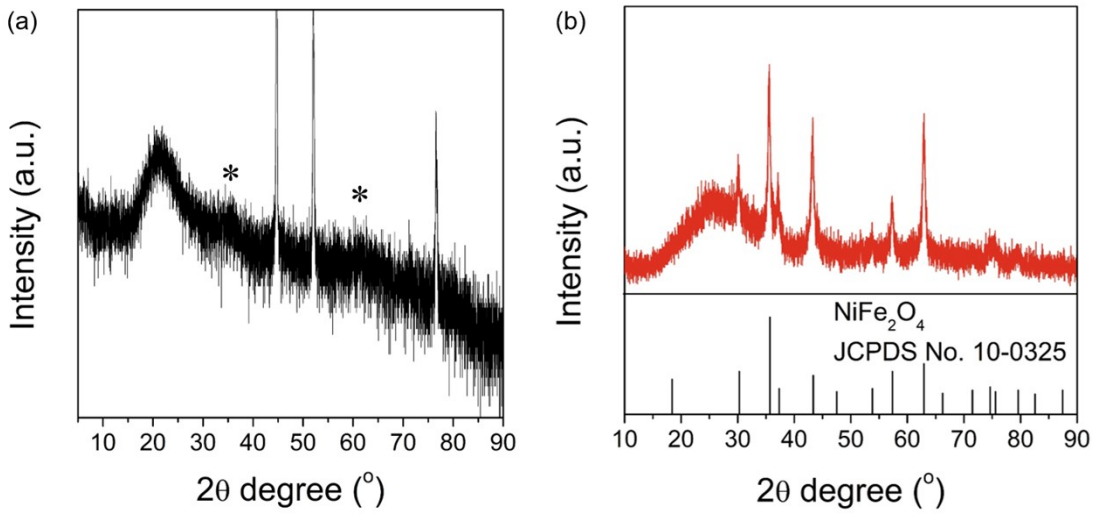

Figure S4 (a) XRD pattern of $NiFeO_x$–1200/NF. The Y axis is in logarithmic scale and the crystalline powder is marked by asterisk. (b) $NiFeO_x$–800 powder sample after calcination in air at 550 °C for 2.5 h.

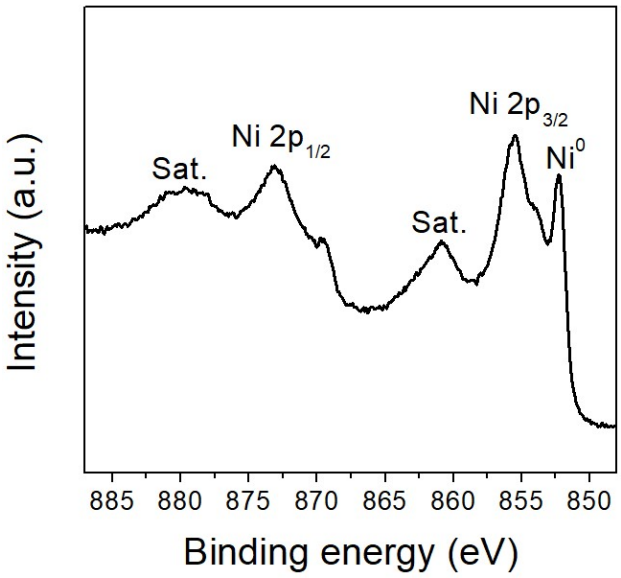

Figure S5 XPS Ni 2p spectrum of NF. The peak at 852.3 eV is indicative of metallic Ni in spite of the presence of slightly oxidized Ni at the surface.

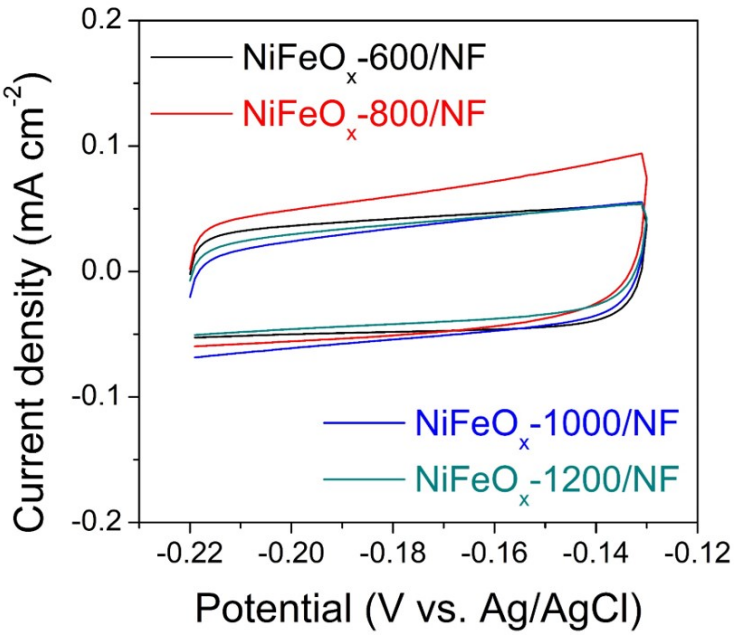

Figure S6 CV curves of $NiFeO_x$/NF prepared via different electrodeposition time (electrolyte: 0.1 M KOH; scan rate: 50 mV s^{-1}).

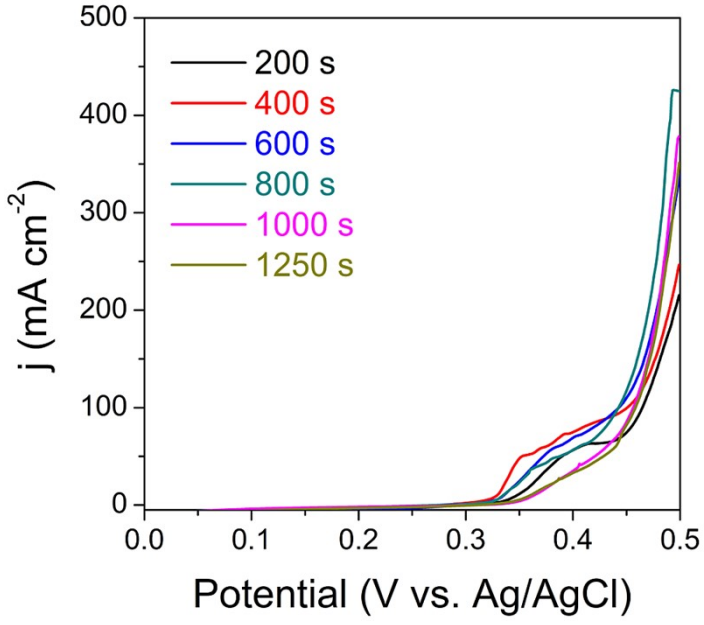

Figure S7 LSV curves $NiFeO_x$–*t*/NF via different electrodeposition time in 1 M KOH at a scan rate of 5 mV s^{-1}.

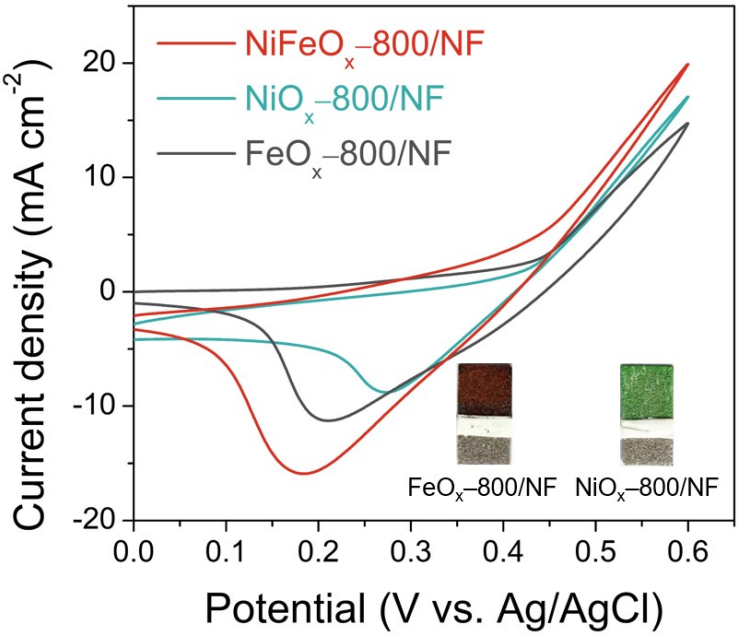

Figure S8 CV curves of NiO_x–800/NF, FeO_x–800/NF and $NiFeO_x$–800/NF (electrolyte: 0.1 M KOH; scan rate: 100 mV s^{-1}). Inset: photographs of FeO_x–800/NF and NiO_x–800/NF.

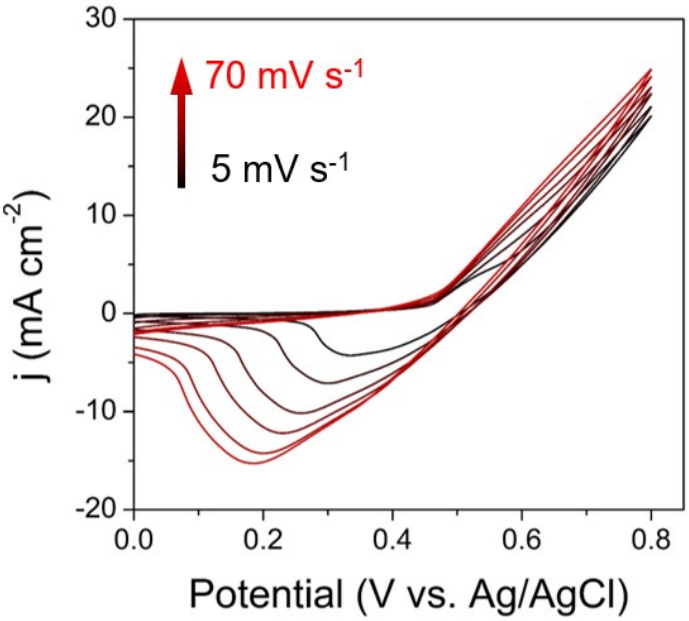

Figure S9 CV curves of $NiFeO_x$–800/NF in 0.1 M KOH + 3 mM glucose at the scan rates from 5 to 70 mV s^{-1}.

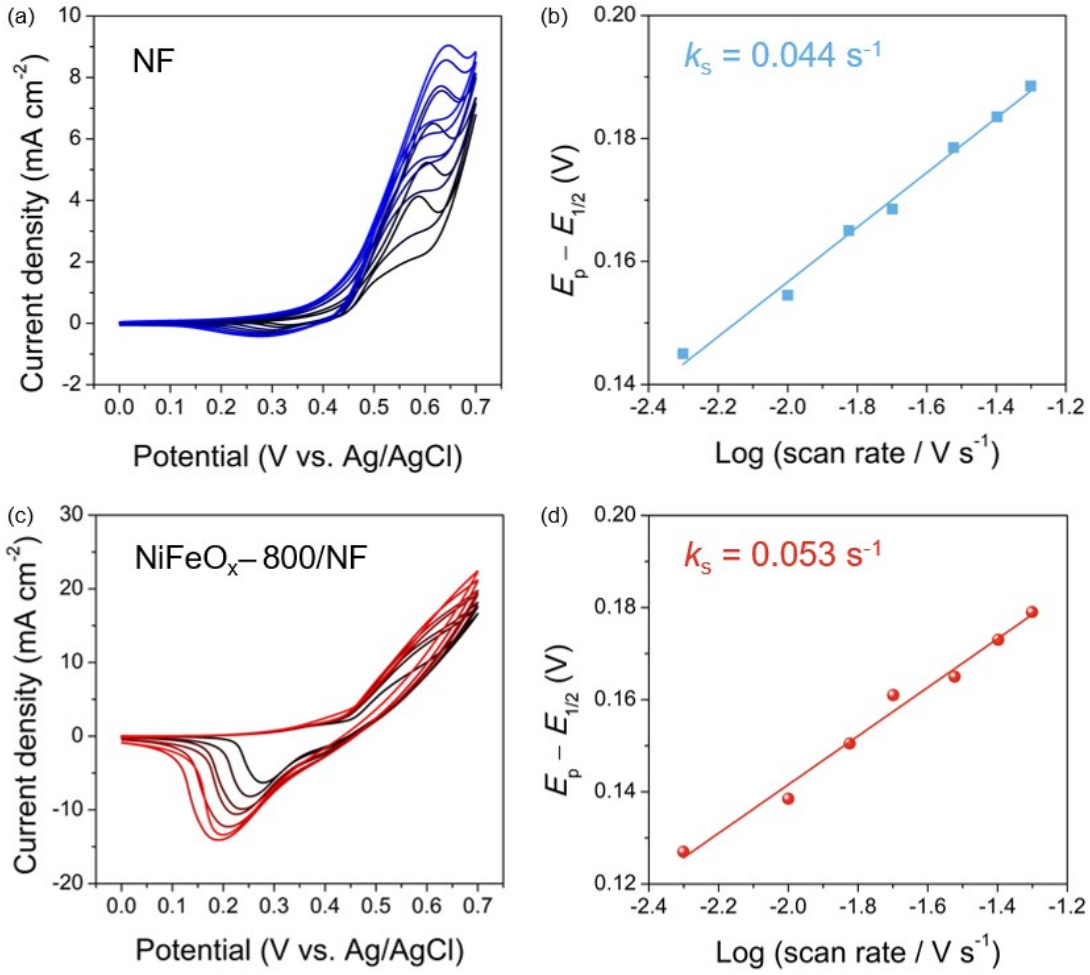

Figure S10 CV curves at the scan rate from 5 to 70 mV s^{-1}: (a) NF and (c) $NiFeO_x$–800/NF Plot of plot of the redox peak potentials versus the logarithm of scan rates: (b) NF and (d) $NiFeO_x$–800/NF.

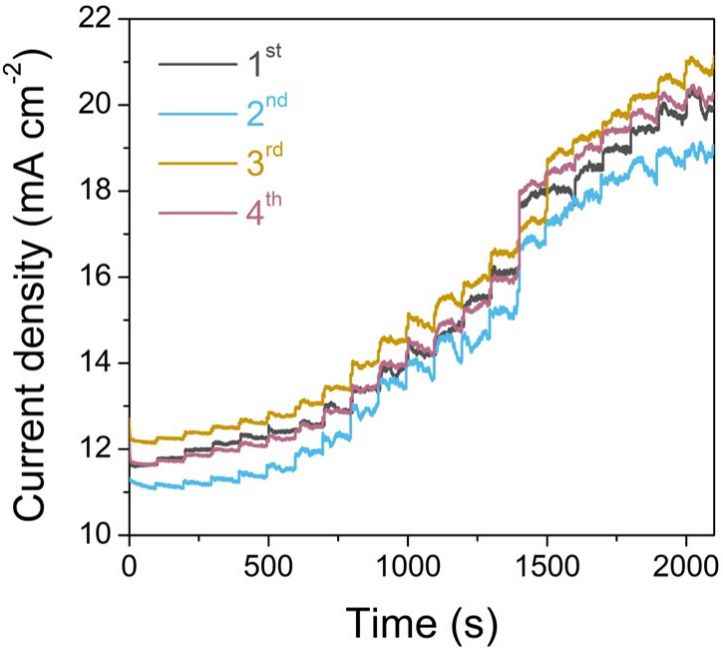

Figure S11 Four *j-t* curves of $NiFeO_x$–800/NF tested at 0.65 V with continuous addition of glucose in 0.1 M KOH solution.

Table S1 Sensitivity comparison between $NiFeO_xH_y$–800/NF and reported materials.

Samples	Sensitivity (μA mM^{-1} cm^{-2})	Year	Ref.
$Co_2N_{0.67}$ nanosheets	921.18	2018	1
Co_3O_4/CC	246.8	2019	2
Ni-N-C	1181	2019	3
Co-Ni-Cu alloy thin film	387	2020	4
CuO/$Ni(OH)_2$	598.6	2020	5
Cu_2O nanocubes	1040	2020	6
Ni_7S_6/$CoNi_2S_4$@CF	2053	2021	7
Cu_2O-Cu-Au	1082	2022	8
CoNi HN@GO	268	2022	9
CuNFs/BDD	2119	2022	10
$NiFeO_x$–800/NF	2320	2022	This work

CC: carbon cloth

CF: carbon fabric

HN: hydroxide nitrate

GO: graphene oxide

CuNFs: Cu nanoflakes

BDD: boron-doped diamond

NF: nickel foam

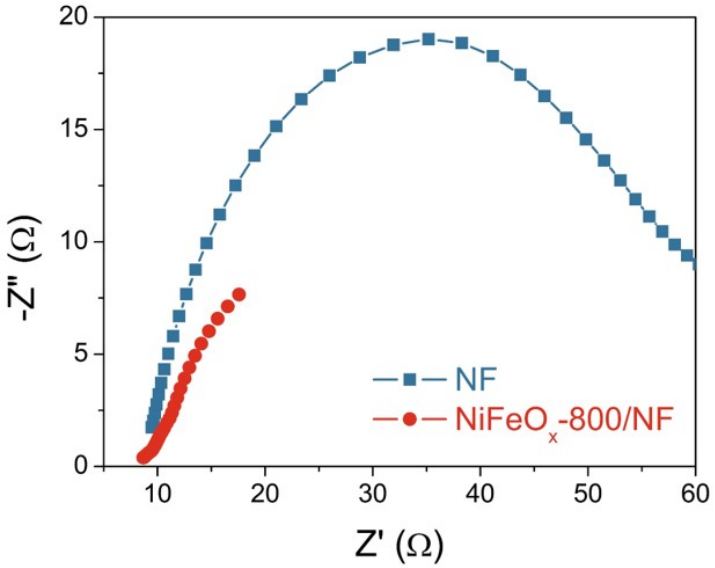

Figure S12 Nyquist plot of NF and $NiFeO_x$–800/NF recorded at potential of 0.5 V.

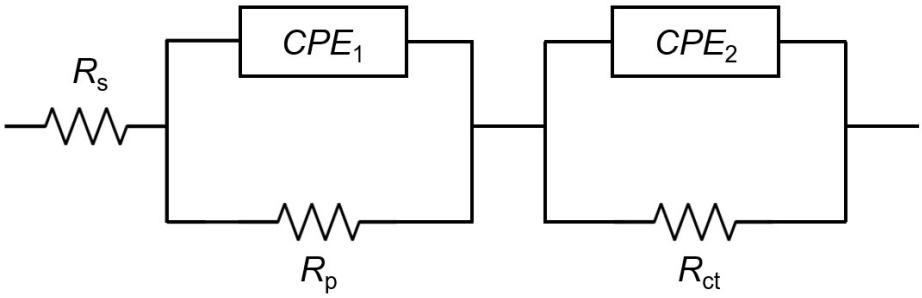

Figure S13 Equivalent circuit model used for EIS data fitting. R_s, R_p and R_{ct} refer to the solution series resistance, resistance of electrode inner film and charge transfer resistance respectively. CPE_1 and CPE_2 stand for the double-layer capacitance and charge transfer capacitance.[11]

Table S2 EIS fitted results of NF and $NiFeO_xH_y$–800/NF at 0.5 V

Samples	R_s (Ω)	R_p (Ω)	R_{ct} (Ω)
NF	8.53	39.02	29.38
$NiFeO_x$–800/NF	8.82	9.12	11.23

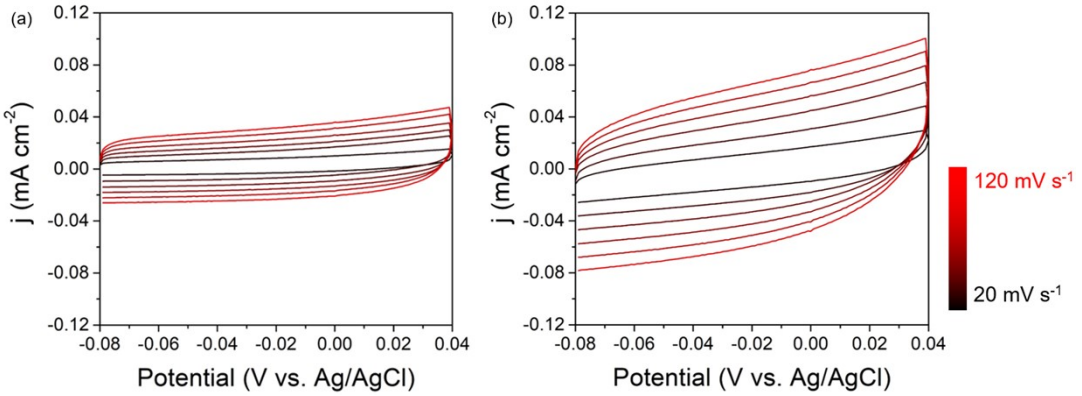

Figure S14 CV curves of NF and $NiFeO_x$–800/NF in the non-Faradic potential range. The scan rate increased from 20 to 120 mV s^{-1} and the electrolyte was 0.1 M KOH and 3 mM glucose.

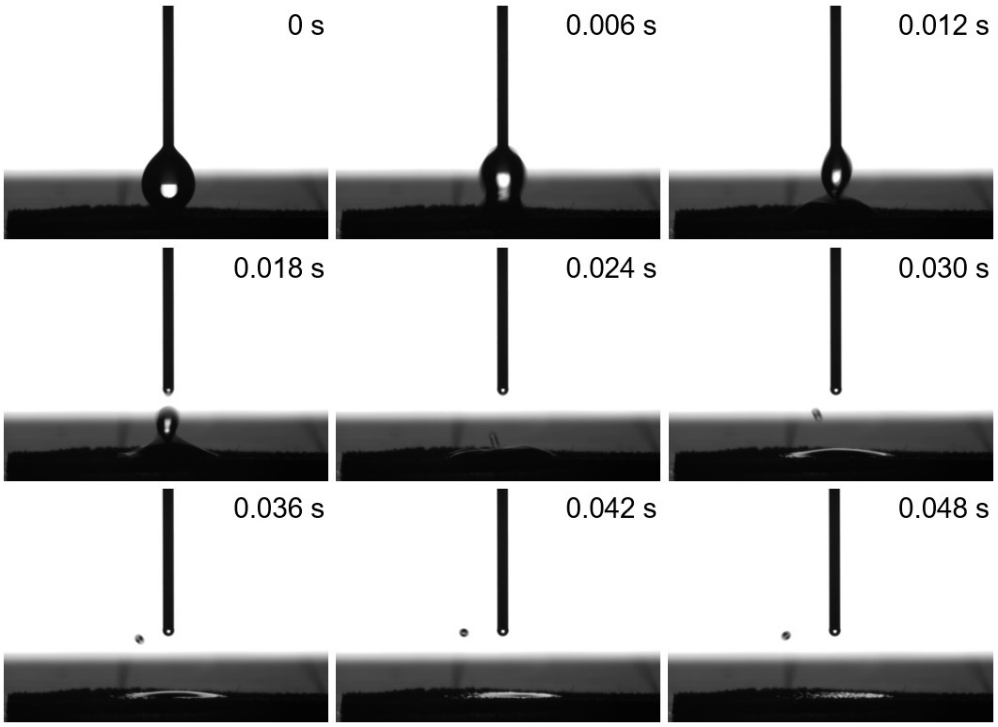

Figure S15 The detailed photographs of water contact angle measurement of $NiFeO_x$–800/NF within 0.05 s.

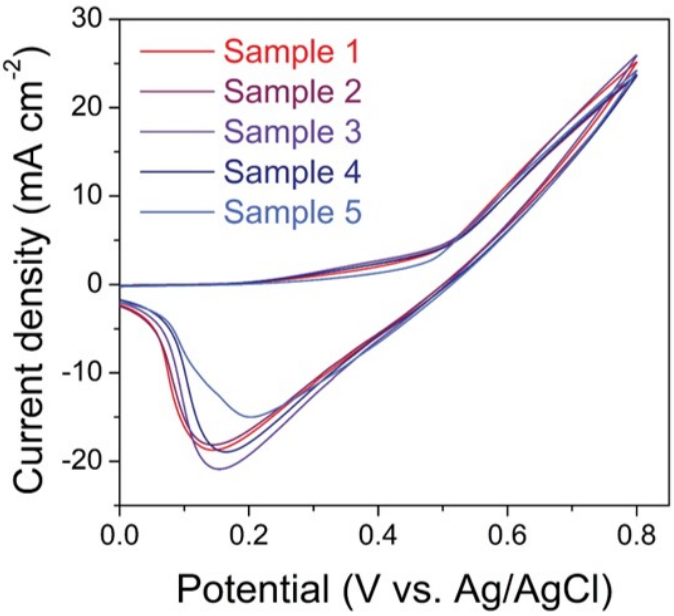

Figure S16 CV curves of five electrodes tested in 0.1 M KOH + 3 mM glucose at a scan rate of 100 mV s^{-1}.

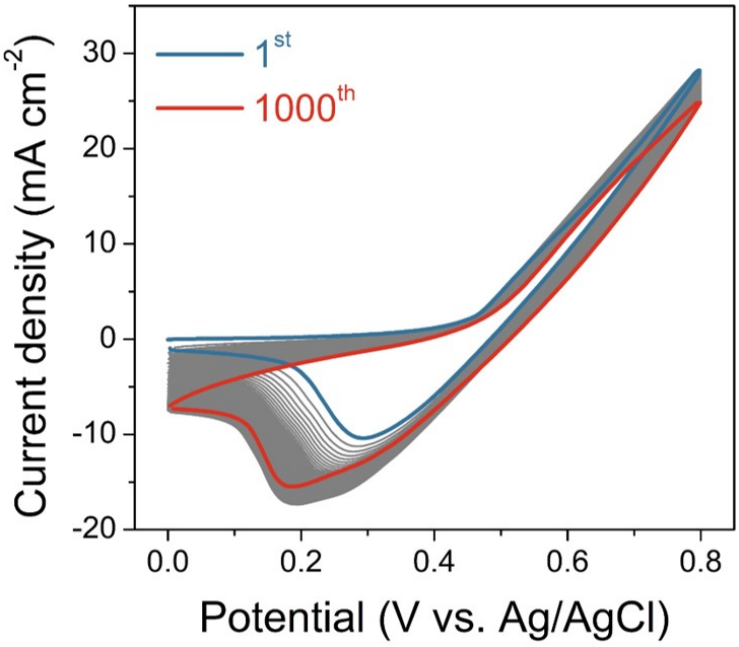

Figure S17 1000 CV curves of $NiFeO_x$–800/NF in 0.1 M KOH + 3 mM glucose at a scan rate of 100 mV s^{-1}.

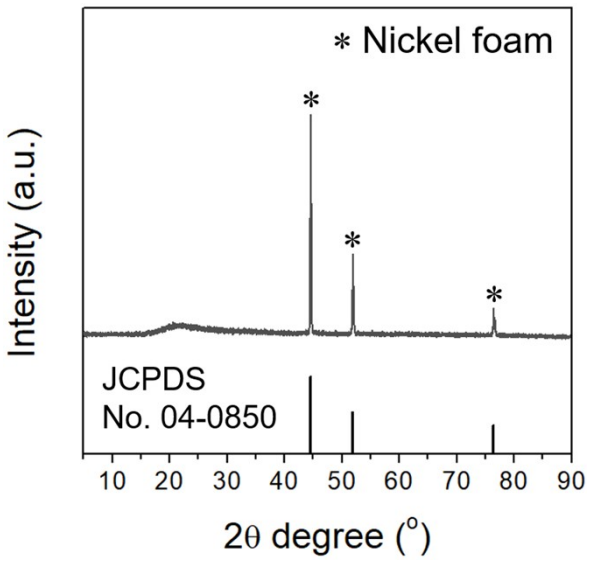

Figure S18 XRD pattern of $NiFeO_x$–800/NF after repeated 1000 cycling tests. Only diffraction peaks of nickel foam can be detected.

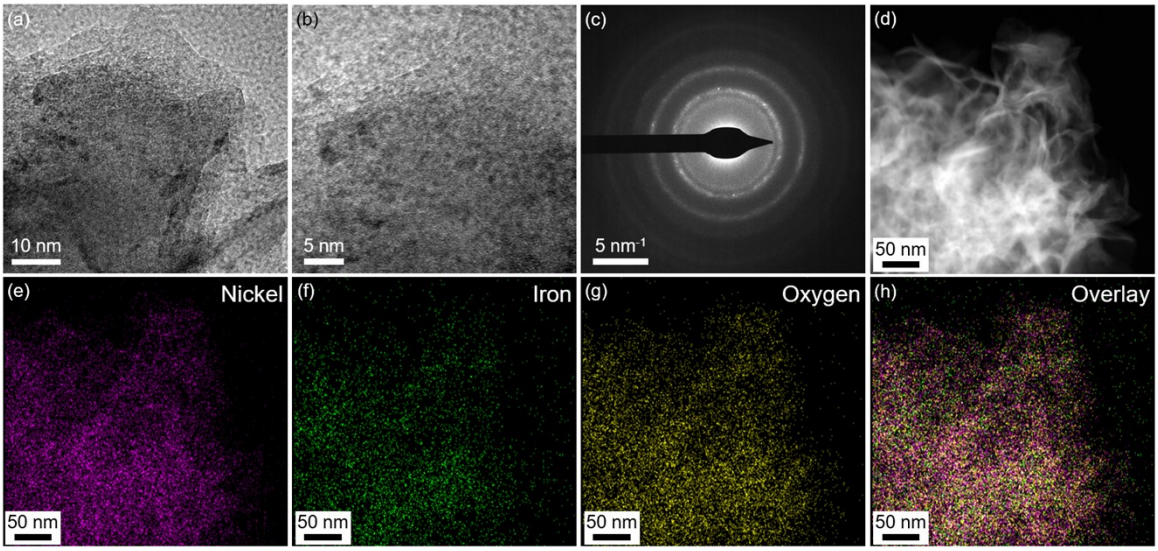

Figure S19 (a, b) TEM images and (c) SAED image of $NiFeO_x$–800/NF after repeated 1000 cycling tests. Elemental mapping: (d) dark-field image, (e) nickel, (f) iron, (g) oxygen and (h) overlay.

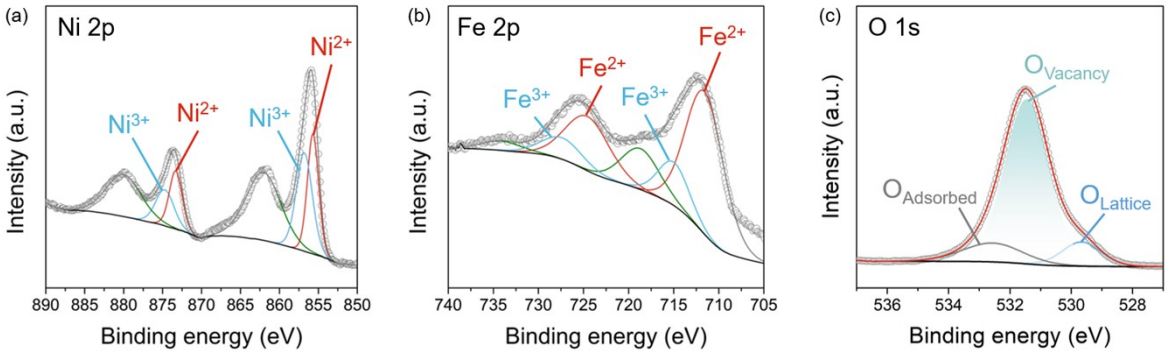

Figure S20 XPS spectra of $NiFeO_x$–800/NF after repeated 1000 cycling tests: (a) Ni 2p, (b) Fe 2p and (c) O 1s spectra.

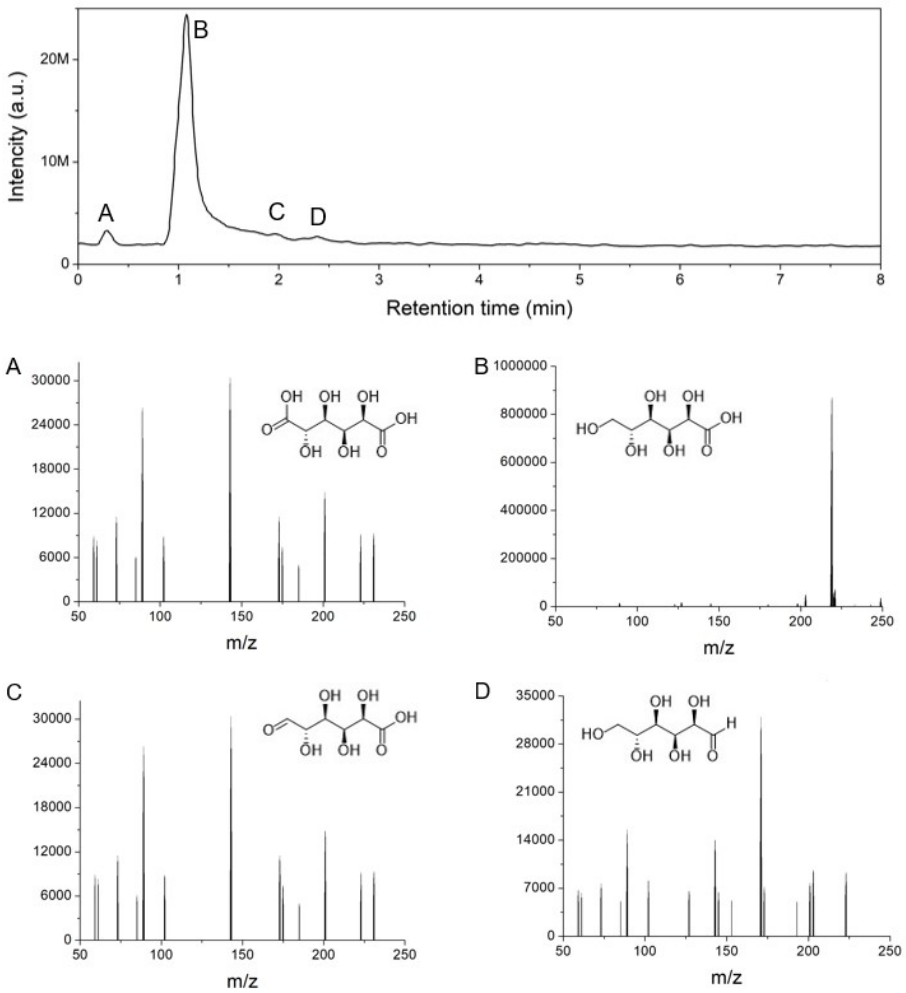

Figure S21 LC-MS analysis of the solution after 1000 glucose sensing CV test (initial glucose concentration: 0.3 M).

Table S3 Analysis of LC-MS results.

	Compounds	Formula	Molecular mass	Main ion stream
A	Glucaric acid	$C_6H_{10}O_8$	210	200 ($M+NH_4^+$+CO)
B	Gluconic acid	$C_6H_{12}O_7$	196	219 ($M+Na^+$)
C	Guluronic acid	$C_6H_{10}O_7$	194	172 ($M+Na^+$-CO—OH^-)
D	Glucose	$C_6H_{12}O_6$	180	203 ($M+Na^+$)

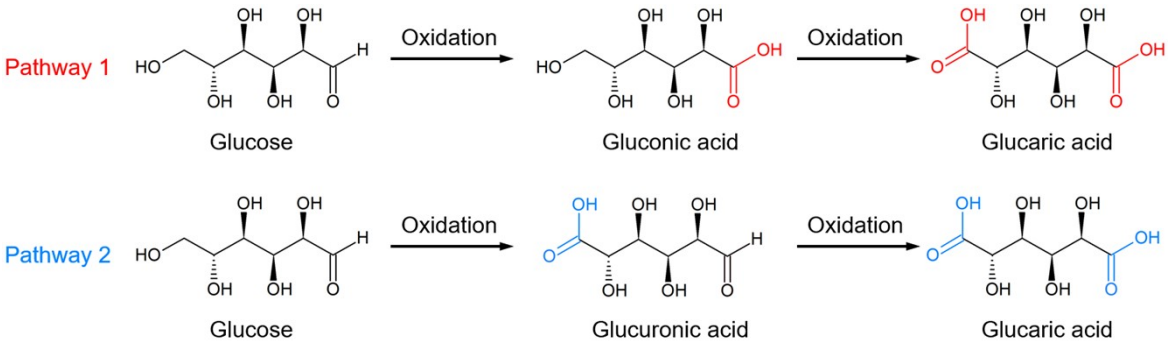

Figure S22 Two possible reaction pathways for glucose oxidation to gluconic acid and glucaric acid.

Table S4 Carbohydrate concentration in commercially available beverages and the corresponding electrochemical current response using $NiFeO_x$–800/NF electrode.

Beverages	Initial pH value	pH value after injecting into PBS solution	Maximum available concentration (g mL^{-1})	Average value of current response (mA) at the testing time of 100 s	Error bar
Lemon juice	3.14	7.13	0.130	0.051	0.0002
Watermelon juice	3.62	7.15	0.129	0.044	0.0004
Mixed juice	3.63	7.16	0.080	0.037	0.0024
Grape juice	2.90	7.14	0.070	0.032	0.0006
Milk	6.60	7.19	0.047	0.022	0.0008

PBS solution was prepared by mixing 200 mL NaH_2PO_4 (0.2 mol L^{-1}) and 50 mL Na_2HPO_4 (0.2 mol L^{-1}).

The pH value of as-prepared PBS solution is 7.20.

The average value of current response is recorded at the testing time of 100 s when the test is stable.

Table S5 The glucose detection of $NiFeO_x$–800/NF in lemon juice.

Samples	Added (mM)	Detection (mM)	Recovery (%)
1	0.1	0.0995	99.50
2	0.2	0.2009	100.49
3	0.3	0.3004	100.13
4	0.4	0.4012	100.30
5	0.5	0.4980	99.60
6	0.6	0.6005	100.08

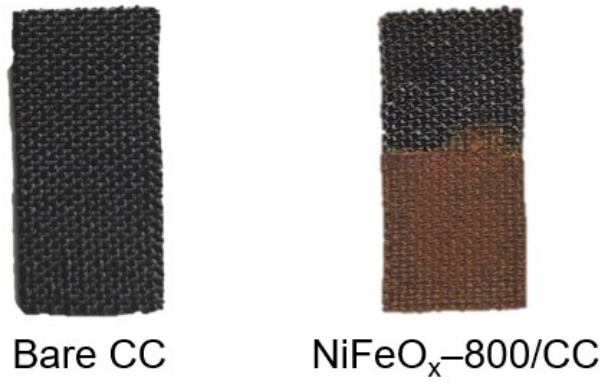

Figure S23 Photographs of bare CC and NiFeO$_x$–800/CC.

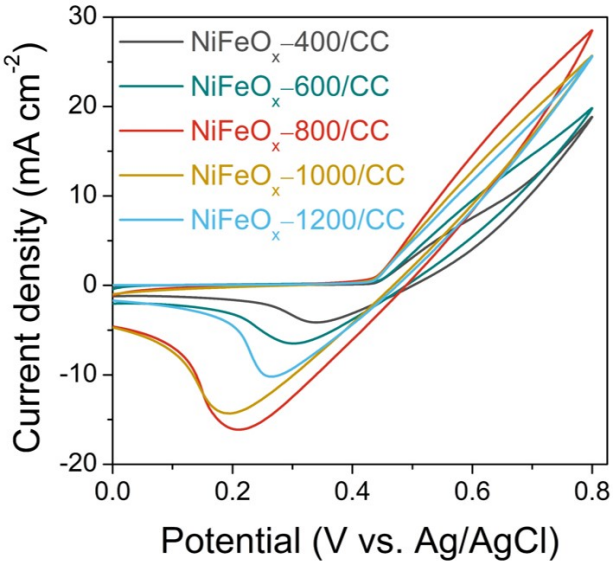

Figure S24 CV curves of NiFeO$_x$–*t*/CC in 0.1 M KOH + 3 mM glucose at 100 mV s^{-1}. *t* stands for the electrodeposition time.

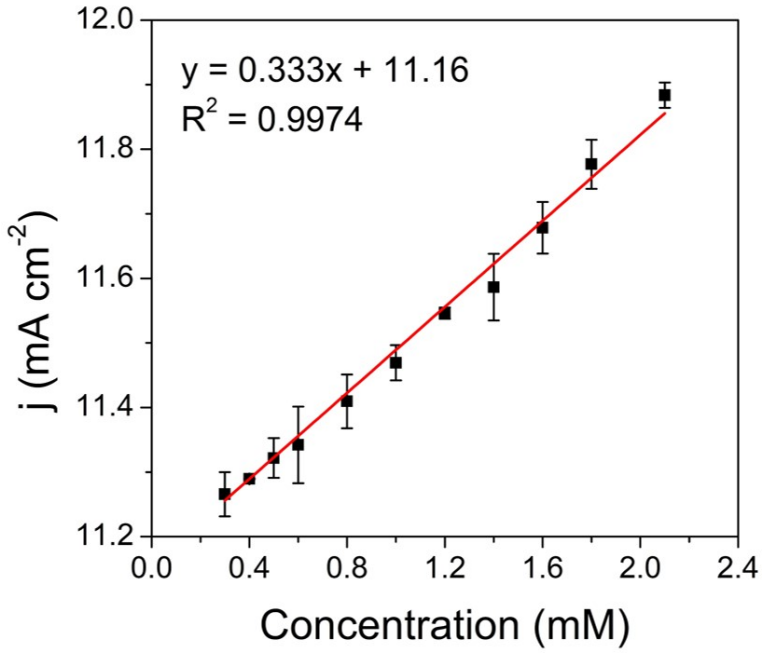

Figure S25 Current density response of $NiFeO_x$–800/CC at 0.65 V to the varied glucose concentration.

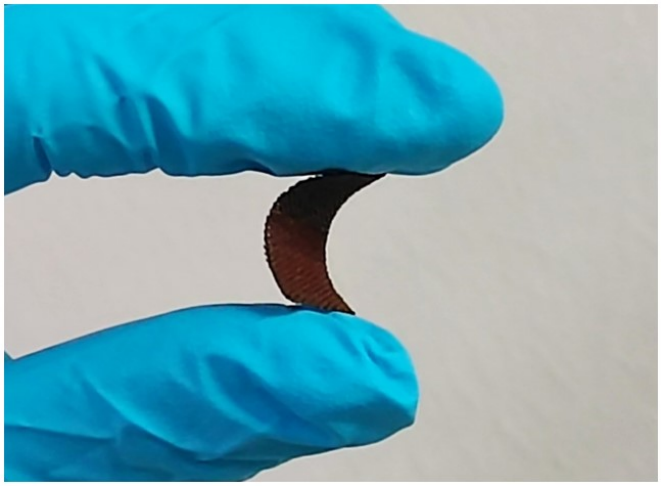

Figure S26 Photographs of $NiFeO_x$–800/CC under bent condition.

References

1. T. Liu, M. Li, P. Dong, Y. Zhang and L. Guo, *Sens. Actuators B: Chem.*, 2018, **255**, 1983-1994.
2. J. Xu, F. Li, D. Wang, M. H. Nawaz, Q. An, D. Han and L. Niu, *Biosens. Bioelectron.*, 2019, **123**, 25-29.
3. X. Chen, X. He, J. Gao, J. Jiang, X. Jiang and C. Wu, *Sens. Actuators B: Chem.*, 2019, **299**, 126945.
4. I. Pötzelberger, C. D. Grill, L. M. Uiberlacker, A. I. Mardare, S. Hild and A. W. Hassel, *Electrochim. Acta*, 2020, **341**, 135744.
5. S. Sun, N. Shi, X. Liao, B. Zhang, G. Yin, Z. Huang, X. Chen and X. Pu, *Appl. Surf. Sci.*, 2020, **529**, 147067.
6. C. Espro, S. Marini, D. Giusi, C. Ampelli and G. Neri, *J. Electroanal. Chem.*, 2020, **873**, 114354.
7. H. Zhao, L. Tang, M. Zhou, K. Li, J. Hu, Y. Zhao and Z. Cai, *J. Mater. Chem. C*, 2022, **10**, 2988-2997.
8. F. Pu, H. Miao, W. Lu, X. Zhang, Z. Yang and C. Kong, *Appl. Surf. Sci.*, 2022, **581**, 152389.
9. S. Gayathri, P. Arunkumar, J. Kim and J. H. Han, *ACS Sustainable Chem. Eng.*, 2022, **10**, 1689-1701.
10. Q. Gao, W. Zhang, C. Zhao, W. Yan, S. Han, Y. Li, Q. Liu, X. Li and D. Liu, *Adv. Mater. Interfaces*, 2022, 2200034.
11. Y. Teng, X. D. Wang, J. F. Liao, W. G. Li, H. Y. Chen, Y. J. Dong and D. B. Kuang, *Adv. Funct. Mater.*, 2018, **28**, 1802463.